RF performance of short channel graphene field-effect transistor

RF Performance of Short Channel Graphene Field-Effect Transistor

Y.Q. Wu[1], Y.-M. Lin[1], K.A. Jenkins[1], J.A. Ott[1], C. Dimitrakopoulos[1], D.B. Farmer[1], F. Xia[1], A. Grill[1], D.A. Antoniadis[2] and Ph. Avouris[1]
[1]IBM T. J. Watson Research Center, Yorktown Heights, NY 10598, U.S.A
[2]Massachusetts Institute of Technology, Cambridge, MA 02139, U.S.A

Introduction: Graphene, a two dimensional single sheet of carbon atoms with excellent electronic properties, has attracted tremendous research efforts because of its high carrier mobility and velocity [1-6]. While the lack of a bandgap in graphene makes its use challenging for digital applications, significant progress has been made on graphene analog devices for radio-frequency (RF) applications, where a high on/off ratio is not necessarily required. Recently, graphene RF transistors [6-7] with a cut-off frequency as high as 100 GHz have been demonstrated [3]. Future advances in the RF performance would rely on the proper scaling of the graphene channel. Despite extensive theoretical efforts, a systematic experimental scaling study has been largely lacking. In this paper, we present experimental studies on transport characteristics of graphene FETs with channel lengths down to 70 nm. The factors limiting the performance of short channel graphene devices are discussed. RF performance of a sub-100 nm graphene transistor fabricated on epitaxial graphene grown on a SiC substrate is also presented. A cut-off frequency as high as 170 GHz is achieved in a 90 nm graphene FET using a scalable top-down fabrication processes. Our results indicate that further improvement of RF performance of graphene FETs can be enabled by channel length scaling with structure optimization and contact resistance reduction.

Experiments: 20nm Pd/30nm Au by e-beam evaporation is used as the contact metal. NFC/HfO_2 is used as the top gate dielectric for top-gated RF devices [3].

Results and discussion: The carrier density dependence of the total resistance of a 1μm and a 70 nm device at V_{ds} =10 mV at room temperature is shown in Fig. 2 and Fig. 3. The mobility can be extracted by model fitting [8]. The quantum capacitance and the impact of gate field on contact resistance are not considered here. Fig. 4 and Fig. 5 show the output characteristics of the 1μm and 70 nm device at room temperature and low temperature. Fig. 6 summarizes the temperature-dependent transfer characteristics for the 70 nm device. The transconductance is increased by almost 40% when measured at low temperature as shown in Fig. 7. Fig. 8 summarizes the temperature dependence of carrier mobility. The decrease of effective mobility as the channel gets shorter is a strong signature of quasi-ballistic transport. [10-12]. Fig. 9 summarizes the temperature dependent contact resistance of the three different devices. The reduction of contact resistance would greatly benefit the DC and RF performance, especially for short channel devices. In order to evaluate the performance of short channel graphene devices for RF applications, a "virtual source" model, which was originally developed for Si MOSFET [9], is adopted here after incorporating the effect of residual doping at the Dirac point, drain-induced doping effect at high drain bias, and the carrier density relation with gate voltage for graphene FETs. The parameters such as contact resistance, mobility and residual doping used in this model are based on the values extracted from the low-field mobility fitting as shown in Figs. 2 and 3. As shown in Fig. 10 and Fig. 11, excellent agreement is obtained between simulation and experimental results for both the transfer and output characteristics of the 70 nm device. The impact of the contact resistance can be witnessed in Fig. 12, where a simulated output characteristic for this device with zero series resistance is shown, exhibiting greatly improved on-current as well as the saturation behavior. As shown in Fig. 13, transconductance can be improved by 4 times for the 70 nm device by reducing the contact resistance, which is much more significant than the long channel case. Fig. 14 shows the RF device fabricated on epitaxial graphene grown on the Si-face of a SiC wafer. The gate length is 90 nm, and the ungated channel length between source and drain is roughly 80 nm. Fig. 16 shows the dc transfer characteristic of the 90–nm-gate graphene FET. The cut-off frequency of this device is as high as 170 GHz at a drain voltage of 2.2V as shown in Fig. 17. It is noted that the device performance here is limited by the series resistance, including the contact resistance and the access resistance associated with ungated region. It is expected that the cut-off frequency can be enhanced to as high as 350 GHz for this 90-nm gate length using a self-aligned gate structure.

Conclusion: We have experimentally demonstrated the high performance short channel RF graphene device with cut-off frequency of 170 GHz on epitaxial graphene on SiC. We have also studied performance improvement by reducing contact resistance at lower measurement temperature for short channel device. The study shows continuous performance improvement can be achieved by proper channel length scaling and structure optimization such as self-aligned gate and technological solutions for contact resistance reduction.

Acknowledgement: The authors thank C.Y. Sung for insightful discussions and B. Ek and J. Bucchignano for technical assistance. The work is supported by DARPA under contract FA8650-08-C-7838 through the CERA program.

References:

[1] K.S. Novoselov, et al., Nature **438**, 197 (2005).
[2] Y. Zhang, et al., Nature **438**, 201 (2005)
[3] Y.-M. Lin, et al., Science **327**, 662 (2010).
[4] I. Meric et al., Nature Nanotechnology **3**, 654 (2008).
[5] C. Berger, Science **312**, 1191 (2006).
[6] J. S. Moon et al., *IEEE Electron Device Lett.,* **31**, 260 (2009).
[7] I. Meric et al., IEDM Digest 4796738 (2008)
[8] S. Kim et al., Appl. Phys. Lett. **94**, 062107 (2009)
[9] D.A. Antoniadis et al., IBM J. Res & Dev. **50** 363 (2006)
[10] M. S. Shur, *IEEE Electron Device Lett*., **23**, 511 (2002)
[11] A. Rahman et al., *IEEE Trans. Electron. Devices*, **50**, 1853 (2003)
[12] Z. Chen et al., *IEDM Tech. Dig.*, 4796737 (2008).

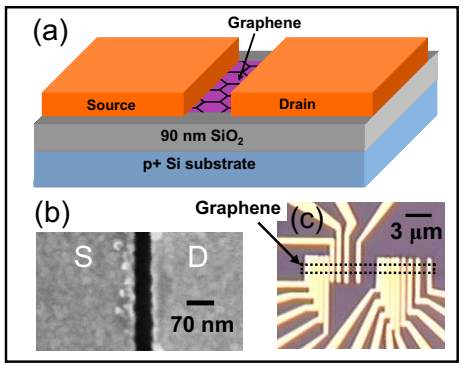

Fig. 1 (a) Schematic view of a back-gated graphene FET, (b) SEM image of metal contacts of a 70nm device and (c) optical image of the fabricated devices.

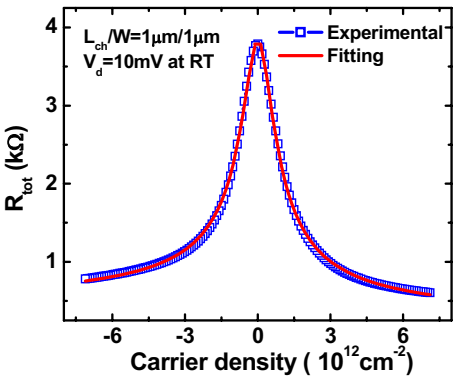

Fig. 2 R_{tot} vs $n_{carrier}$ of a 1μm device at 10 mV at room temperature and the fitting based on Eq. (1). The C_g used here is calculated from the 90 nm SiO_2.

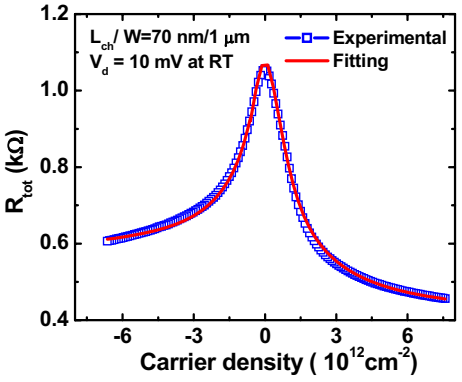

Fig. 3 R_{tot} vs $n_{carrier}$ of a 70 nm device at 10 mV at room temperature and the fitting based on Eq. (1) .

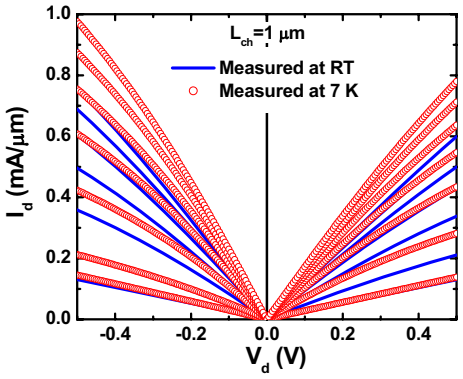

Fig. 4 Output characteristics for a 1μm device at room temperature and 7 K. V_{bg} sweeps 30 V from Dirac point with a step of 5 V for both nFET and pFET.

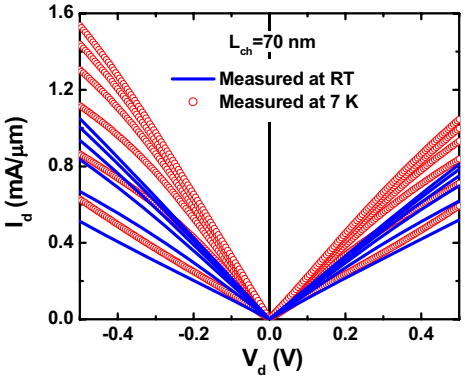

Fig. 5 Output characteristics for a 70 nm device at room temperature and 7 K. V_{bg} sweeps 25 V from Dirac point with a step of 5 V for both nFET and pFET.

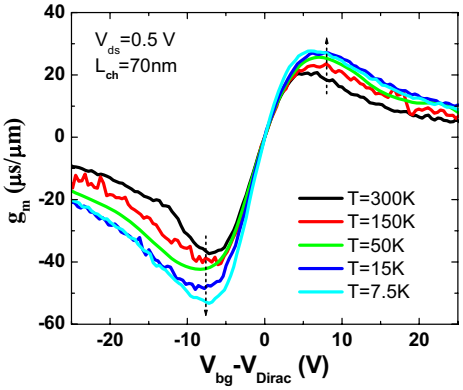

Fig. 6 Temperature dependent transconductance for a 70 nm device.

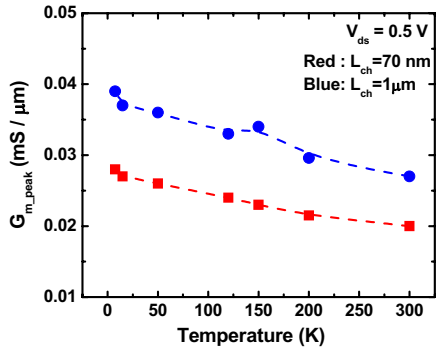

Fig. 7 Peak transconductance g_m vs. T from devices with channel length of 1 μm and 70 nm.

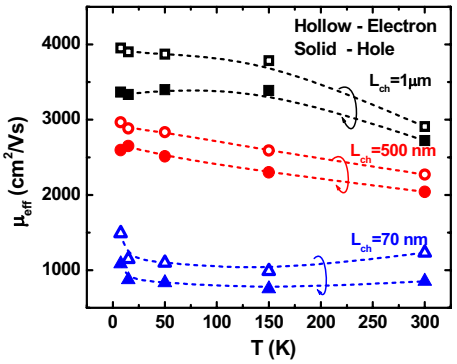

Fig. 8 Effective electron and hole mobility μ_{eff} vs. T from devices with different channel length, from 1 μm down to 70 nm.

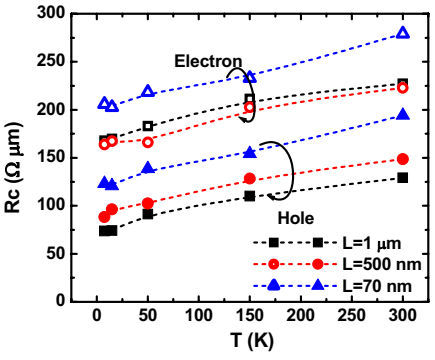

Fig. 9 Contact resistance R_C vs. T from devices with different channel length, from 1 μm down to 70 nm.

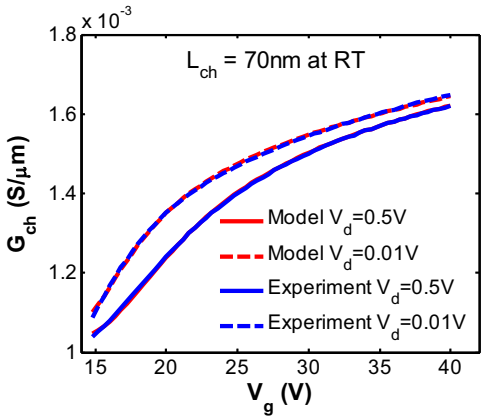

Fig. 10 Comparison of experiment and model of the transfer characteristics of a 70 nm device at room temperature.

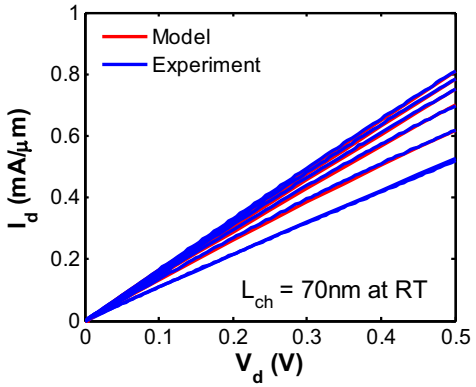

Fig. 11 Experimental output characteristic and model for a 70 nm device at RT. V_{bg} sweeps 25V from Dirac point with a step of 5 V.

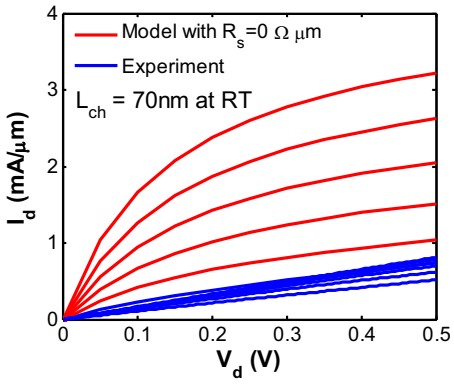

Fig. 12 Modeled output characteristics with R_s=0 for the 70nm device at RT. V_{bg} sweeps 25V from Dirac point with a step of 5 V.

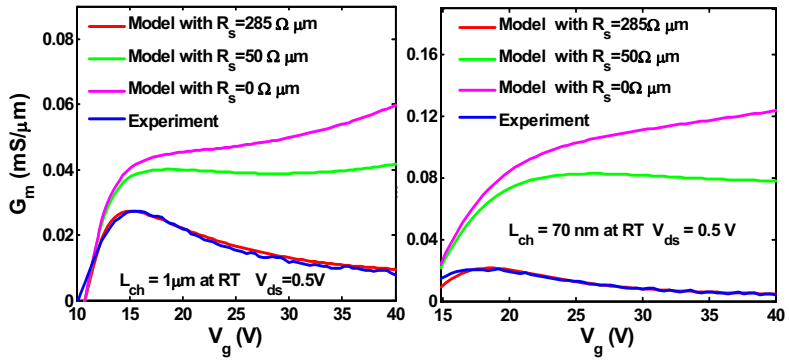

R_S (Ω μm)	285	50	0
f_T (GHz) L_{ch}=1 μm	10.8	16.6	24.9
f_T (GHz) L_{ch}=70nm	118.4	485.5	728.3

Fig. 13 Modeling of G_m by varying R_s for 70 nm and 1μm devices and the improvement of projected f_T.

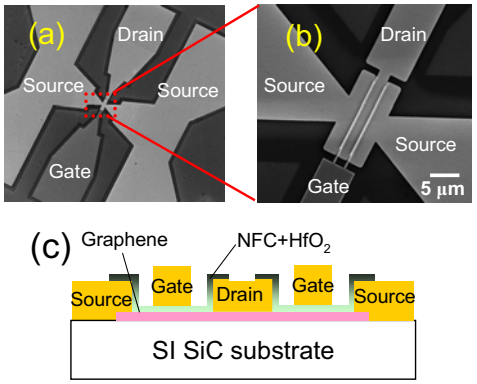

Fig. 14 SEM image of a finished RF device (a&b) Schematic view of a top-gated RF graphene FET (c) .

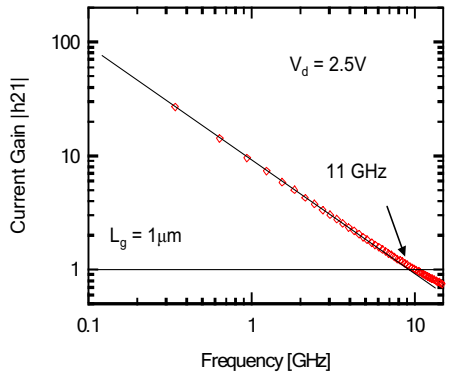

Fig. 15 A RF graphene transistor showing a cut-off frequency of 11 GHz. The gate length is 1 μm.

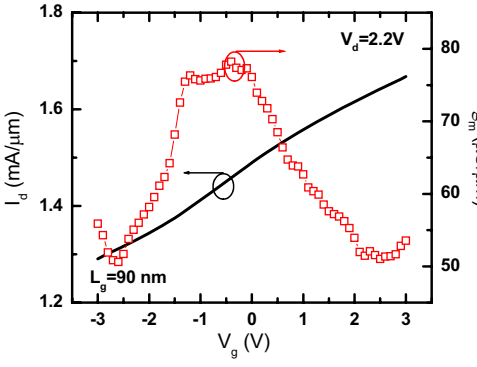

Fig. 16 Transfer characteristics of a short channel RF graphene devices at V_{ds}=2.2 V.

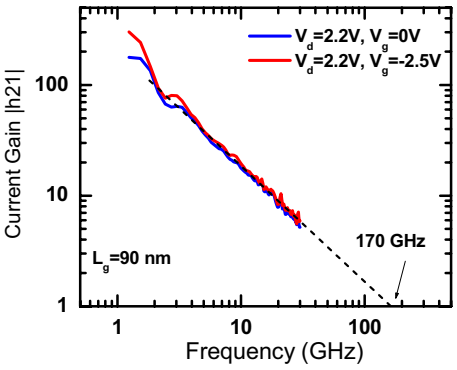

Fig. 17 A high performance graphene transistor showing a cut-off frequency of 170 GHz. The gate length is 90 nm.